Structural acoustics of good and bad violins

George Bissinger[a)]

Physics Department, East Carolina University, Greenville, North Carolina 27858, USA

Modal-acoustic radiation measurements on 17 "bad-to-excellent" quality-rated violins—including three-dimensional modal analyses of *Titian* and *Willemotte* Stradivari and *Plowden* Guarneri del Gesu violins to investigate *extensional* as well as flexural motions—were examined for quality-related trends, generally by contrasting the properties of "excellent" and "bad" violins. All violins tested showed the same five "signature" modes below 600 Hz, with no obvious quality trends for mode frequencies or total damping. Bad–excellent comparisons of band-/modal-averaged damping (total, radiation and internal), mobility, radiativity, directivity, fraction-of-vibrational-energy radiated, effective critical frequency, and radiativity profiles up to 4 kHz generally showed no significant difference; the only "robust" quality differentiator was the ~280 Hz, Helmholtz-type A0 cavity mode radiativity where excellent violins were significantly higher. Radiation and total damping of two old Italian violins appeared slightly higher than those for bad violins below 2 kHz, partly due to lower effective critical frequency and partly because of slightly lower mass. Stradivari violins showed the highest and lowest directivity of all instruments tested. The *Titian* and *Plowden* top plate flexural/extensional mobility ratios appeared correlated with their directivity. Extensional motion in the "bridge island" between *f* holes peaked near 2.4 kHz, coinciding with the BH peak and a bridge/bridge-island impedance ratio minimum. © *2008 Acoustical Society of America.* [DOI: 10.1121/1.2956478]

Pages: 1764–1773

I. INTRODUCTION

A robust relationship between perceived violin quality and various mechanical–acoustical parameters amenable to scientific measurement has been an elusive scientific goal for almost two centuries. However, in the 1980s the advent of experimental modal analysis, near-field acoustical holography, zero-mass-loading excitation-response transducers, finite element and boundary element method computational techniques along with CT scan technology (to provide shape and density information)—all relying on the concurrent, equally rapid development of the computer—provided entirely new, and comprehensive ways to characterize the violin's dynamic and material properties. For the first time in the history of violin research it became possible to understand the surface vibratory behavior and motion of air in the *f* holes in great detail based on individual normal mode characterizations, or statistically via modal or band averages, accompanied by the potential to simulate these very vibrations.[1–11] Each violin mode could be characterized by mode shape, frequency, total damping (similarly for its major substructures, the top and back plate), and character (corpus bending modes, cavity, coupled cavity corpus, etc.), as well as by its acoustic radiation properties, e.g., radiation efficiency.

Such extensive and detailed information has led to some interesting simplifications, e.g., irrespective of quality, all traditional violins (and a complete violin octet[7]), properly constructed and set up, have only five "signature" corpus (top+ribs+back) normal modes in the open string region—

albeit sometimes tailpiece or neck-fingerboard substructures can couple to these modes, splitting them. The violin's open string region (196–660 Hz for A=440 Hz) is crucial to the sound of the violin and also where the lowest plate modes are most important. Above ~700 Hz when the violinist holds/plays the violin the total damping increases so much that mode overlap suggests more statistical modal-/band-average analyses. Combining modal analysis with far-field acoustic radiativity measurements expands the descriptive structural acoustics parameters to radiation efficiency, radiation damping, internal damping, fraction-of-vibrational-energy radiated, and effective critical frequency.[11]

Add to this expanded range of parameters true three-dimensional (3D) modal analyses over a wide frequency range to examine a very important—but almost completely neglected—area of violin vibratory behavior, viz., in-plane extensional motion versus flexural out-of-plane motion. (To date only one investigation of these motions has been made, at a few fixed frequencies in the 400–600 Hz range.[12]) Although extensional motion does not lead directly to acoustic radiation, extensional motion can be transformed into flexural motion (and vice versa) at boundaries or discontinuities. The use of curved shells rather than flat plates for the violin's top and back implies significant extensional motion, hence the intractable analytical problem of determining relative contributions of flexural versus extensional motion for complicated shapes like the violin was approached experimentally in a straightforward way to provide a direct insight into the way the violin partitions its vibrational energy, which in turn is linked to its radiative properties. Of exceptional importance in this regard is the boundary-discontinuity concentration in the "bridge island" between *f* holes, where the

a)Electronic mail: bissingerg@ecu.edu.

soundpost, bass bar, and the *f* holes themselves are situated in the very region where string energy enters the corpus through the bridge feet.

This work, summarizing almost 10 years of wide-ranging vibration and radiation measurements on 17 violins and a complete violin octet, combines one-dimensional (1D) calibrated modal analyses of 12 quality-rated violins (including bridge, tailpiece, and neck-fingerboard substructures), new 3D scans of three old Italian and one modern violin with calibrated acoustical scans over a sphere in an anechoic chamber for all 17 violins, and a CT scan of each violin for density-shape material information. This 17-violin database (hereinafter labeled VIOCADEAS[13]) was mined for possible "robust" empirical parameter–quality relationship trends using a variety of approaches.

II. EXPERIMENT

Previous publications covered all relevant 1D experimental details for the comprehensive violin measurement-simulation program VIOCADEAS (Refs. 9 and 13, and references therein). All vibration measurements utilized zero-mass-loading laser scans of mobility $Y(\omega)$ (complex ratio of velocity/force) at >550 points over the ribs, top–back plates, bridge, neck-fingerboard, and tailpiece (the latter three substructures scanned from two orthogonal directions, creating two-dimensional scans) up to 4 kHz. The substructure (top, ribs, back) spatial-average, mean-square surface-normal mobilities $\langle Y^2 \rangle$ were used here to compute the substructure-area-weighted rms corpus mobility $\langle Y_{corpus} \rangle$. All 1D–3D mobility—and acoustic radiativity $R(\omega)$ (complex ratio of pressure/force)—measurements used zero-mass-loading, force-hammer impact excitation at the G-string corner of the bridge of violins suspended "free–free" from thin elastics (support fixture damping, ≤5% of total damping, was neglected in all analyses).

Far-field radiativity scans at 266 points over an r =1.2 m sphere in an anechoic chamber were made for all 17 violins. An over-the-sphere average of the mean-square radiativity $\langle R^2 \rangle$ was used to compute the rms radiativity $\langle R \rangle$; top and back hemisphere radiativities $\langle R_{top} \rangle$ and $\langle R_{back} \rangle$, respectively, (in-plane microphone points dropped), were used to compute a rough measure of directionality, the directivity $\langle D(\omega) \rangle = \langle R_{top}(\omega) \rangle / \langle R_{back}(\omega) \rangle$.

All violins were measured in playing condition with undamped strings at tension (A=440 Hz) without chin or shoulder rest. Nine of the twelve 1D-scan violins (and the Curtin violin) also had top and back plate mode frequency information provided by the maker. Two of the violins had bent, not carved, plates. Finally, all violins were played by the same violinist (Ara Gregorian) for quality evaluation purposes, although time constraints in the 3D-scan experiment necessitated a more general evaluation procedure for those violins.

The entirely new 3D mobility scans reported here significantly broadened the scope of VIOCADEAS, examining *extensional* as well as flexural surface motion over a broad frequency range. Over the available $2\frac{1}{2}$ day measurement period the *Titian* Stradivari (1715) and *Plowden* Guarneri del Gesu (1735) had essentially complete corpus scans, plus partial scans on the *Willemotte* Stradivari (1734, back plate only) and Joseph Curtin (2006, top plate only), plus a few high-density-point scans at specific frequencies. Corpus 3D scans required much more time than the $3\frac{1}{2}$ h needed for complete 1D grid scans (top, back, ribs, plus neck-fingerboard, tailpiece, and bridge from two orthogonal directions), plus acoustic scans over a sphere because of the prior 3D surface geometry scans needed for each violin to accurately specify *XYZ* coordinates for all points in the 3D measurement grid. Three separate lasers simultaneously measured the surface velocity vector along each laser's beam direction at each point; top plate exclusion zones were somewhat larger than for 1D measurements due to neck-fingerboard, bridge, or tailpiece surface shadowing. The time-limited 3D experiment led to an error of omission in the automated backhemisphere radiativity scans, which covered 0–4 kHz, not 0–5 kHz as in all other 3D measurements. In this article, 1D–3D force hammer excitation was along the *X*-direction only.

The three mobility vectors were then decomposed into orthogonal components in a chosen frame of reference.[14] Since the violin has no flat surfaces, the *Y* direction (perpendicular to the "plane" of the violin)—the component used for comparison with previous 1D measurements on top and back plates—was labeled out-of-plane (OP), and the *XZ* plane labeled in-plane (IP) for convenience. In the bridge "island" between *f* holes, *X* and *Z* mobilities were analyzed separately to understand extensional motion in the crucial region where string energy enters the violin.

III. RESULTS

Mobility spectra provided normal mode frequency, total damping, ζ_{tot}, and mode shapes to characterize each violin's vibrations, whereas radiativity spectra provided directivity as well as radiativity "profiles" useful in characterizing violin sound. Radiation efficiency, R_{eff}, radiation damping, ζ_{rad}, *effective* critical frequency, f_{crit}, and the fraction-of-vibrational-energy-radiated $F_{RAD} = \zeta_{rad}/\zeta_{tot}$ were computed from combined mobility and radiativity measurements. Various approaches were used to examine experimental parameter–quality relationships, e.g., plots of parameter versus quality rating to look for trends, or clumping the violins into "bad," "good," and "excellent" groups for statistical analysis, or applying trend-line analysis to quality-grouped parameters, etc. At low frequencies where individual signature modes were seen for all violins irrespective of quality, mode frequencies and total damping were examined for trends. At higher frequencies mode overlap becomes so pervasive and mode shapes so variable, even for our free–free support, that more statistical band- or modal-average analyses and trend lines—notably to estimate f_{crit}—were utilized. Note that string-peak structures were still obvious and much narrower than the corpus peaks over the entire frequency range. The 3D vibration OP–IP measurements were examined for a possible link to radiation directivity $\langle D \rangle$.

Violin subjective quality ratings were on a 1–10, three-main-class rating scale—bad (1–3), good (4–7), and excel-

lent (8–10). Previously violin parameter versus quality comparisons were between the highest ranking good and the bad violins;[11] the new data on three old Italian violins has extended the quality range to excellent. Thus comparisons have evolved to excellent versus bad comparisons (plus all-violin averages where appropriate) in an attempt to magnify possible differences in quality-related parameters; note that *quality–class* comparisons are stressed rather than individual violin results. Because any analysis of only 17 violins suffers from small-number statistics for the various quality groups, only robust quality quantifiers—where standard deviation error bars did not overlap—will be given much consideration. Even robust quantifiers, however, cannot be considered reliable without extensive corroboration.

A. Mobility and radiativity

1. Signature modes

Our discussion of individual modes will be limited to just those five low-lying modes observed in all measured violins and the violin octet. These signature modes fall into two major classes:

(1) Cavity modes: (a) A0, always the lowest frequency mode, $f_{A0} \approx 280$ Hz. A Helmholtz-type mode characterized as a mass-plug oscillating under the influence of the cavity "spring," always a strong radiator, and (b) A1, the first longitudinal mode, sometimes an important radiator with $f_{A1} \approx 1.7 f_{A0}$. These are *coupled* modes and each has an admixture of the other, a circumstance that strongly affects the A0 volume dependence and the upper–lower bout pressure ratios.[15]

(2) Corpus modes: (a) CBR, the lowest frequency corpus mode with shearlike IP relative motion between top and back plates, a ‡ OP nodal line pattern on top and back plates accompanied by out-of-phase f-hole volume flows and thus relatively weak radiation, and (b) the first corpus bending modes B1⁻ and B1⁺—which both radiate strongly and also strongly through the f holes.[10]

The strongly radiating A0, B1⁻, and B1⁺ modes in the open-string, 196–660 Hz region are crucial to violin sound.

Figure 1 shows the rms corpus OP mobility $\langle Y_{corpus} \rangle$ and rms top hemisphere radiativity $\langle R_{top} \rangle$ for the *Titian* Stradivari and *Plowden* Guarneri del Gesu in the open string region with the signature modes annotated. These radiativity and mobility curves were not exceptional in magnitudes, widths, or peak placements compared to other violins.

2. Magnitudes

The mobility and radiativity magnitudes of bad, excellent, and 14- or 17-violin averages (nominally good violins) are presented in Fig. 2 as 250 Hz band averages, with two important exceptions—"A0" is an average over ±10 Hz around the A0 peak, while the 400 Hz band is averaged from 300 to 499 Hz to exclude A0, but including CBR and B1⁻. All higher bands are over 250 Hz intervals; the band centered at 625 Hz always includes B1⁺. This band choice ensures the lowest three radiativity bands are dominated by A0, B1⁻, and B1⁺, respectively, *Intraband* variations are shown
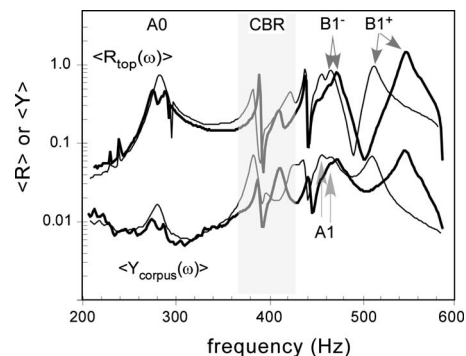

FIG. 1. Signature mode region OP (log) corpus mobility $\langle Y_{corpus} \rangle$ (lower curves, m/s/N) and top hemisphere (log) radiativity $\langle R_{top} \rangle$ (upper curves, Pa/N) for *Titian* Stradivari (thick line) and *Plowden* Guarneri del Gesu (thin line) vs frequency. Note low A0 mobility; narrow structures are string harmonics (always narrower than corpus peaks). *Titian* A0 shows neck-fingerboard or tailpiece coupling.

in Fig. 2 with standard deviation (s.d.) error bars. Radiativity provides an objective measure of how effectively forces applied at the bridge can be turned into sound without any ear sensitivity weighting. Figure 2 clearly shows that the only robust difference between bad and excellent (old Italian) violin radiativity occurs for A0. This does not imply that we may not *perceive* them as louder, or that their directivity is the same. In fact, both aspects are important.

The average mobility falls off smoothly above the maximum near 2.4 kHz, which was originally attributed to the bridge "rocking" about the waist, with the feet relatively fixed. A similar peak has shown up in every part of the energy chain: bridge driving point, averaged-over-bridge, bridge feet, averaged corpus mobility, and radiativity.[16] However experiments by Jansson and co-workers[17] with solid and standard bridges clearly demonstrated that this
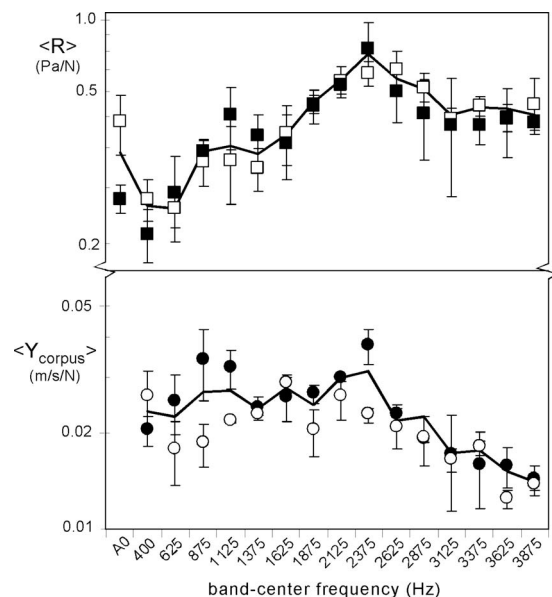

FIG. 2. Top panel: Band-average (log) radiativity $\langle R \rangle$ (17 violins); bottom panel: Band-average corpus OP (log) mobility $\langle Y_{corpus} \rangle$ (14 violins, A0 mobility omitted) vs band-center frequency: "bad"—solid symbol), "excellent"—open symbol (all old Italian), and average—line (here average is nominally "good"). (s.d. error bars reflect *intraband* variations only.)

George A. Bissinger: Structural acoustics good–bad violins

peak did not originate in the bridge rocking about the waist, a conclusion corroborated by an experiment where frequencies for this type rocking were varied widely.[16] This matter of the BH peak will be addressed more thoroughly in a later section on 3D measurements. Corpus mobility showed some evidence of a bad–excellent difference in the 875–1125 and 2375 Hz bands.

The radiativity profile of the bad violins was somewhat more peaked than the excellent, with the A0 and high frequency ends both lower. Overall, excellent violins had a somewhat more uniform response.

B. Violin mode properties versus quality

The following results summarize violin normal mode properties sorted by their subjective quality rating. All violins were played by the same excellent violinist Ara Gregorian; the 12 VIOCADEAS violins' overall ratings used a systematic multiparameter rating scheme, while the Curtin, Zygmuntowicz, Stradivari, and Guarneri del Gesu violins in the 3D experiment were all evaluated in a different way and have numerical ratings supplied by the author based on Gregorian's comments while playing, listeners comments, and in case of the old Italian violins their historical summary status. This qualitative rating should not be considered absolute—in the sense of some other excellent violinist coming to exactly the same numerical value—but as a reasonably reliable evaluation based on a consistent rating scheme. The fact that no robust quality trends emerged from this analysis reflects a reality in trying to quantify violin quality.

1. Signature mode frequency and damping

Schleske, a prominent German violin maker who has been the leader in incorporating modal analyses into violin making, stated[5] that the frequency of B1$^{(+)}$ acts as a "tonal barometer" for violin sound, with frequencies <510 Hz leading to a "somewhat soft" violin with dark sound, lacking "resistance" to bowing. On the other hand frequencies >550 Hz were characteristic of "…'stubborn' violins with bright sound, possibly with a tendency to harshness, and with strong 'resistance' to the player." It is unclear how a 10% change in corpus B1$^+$ frequency could cause such a change in perceived mechanical response since the string terminations are relatively insensitive to corpus vibrations except in the case of wolf-tones. Such "mechanical" characterizations may actually have significant *acoustic* components. Rohloff, in a 1964 experiment where filter-controlled violin sound reached the violinist only through headphones, found that a violin's resistance was linked, not to the bowing force needed to initiate tones as one might expect, but rather to *acoustic strength above* 4 kHz: "easy-speaking" violins had extended response above 4 kHz, "hard-speaking" violins had limited response.[18]

Schleske's remarks, however, do suggest that B1$^+$ frequency might in some way be a convenient gauge of quality, a conjecture readily tested by plotting B1$^+$ and all other signature mode frequencies for all 17 violins versus subjective quality rating in Fig. 3. Overall, A0 averaged 275 ± 9 Hz (s.d. errors: min. 253 Hz, max. 282 Hz), A1 averaged
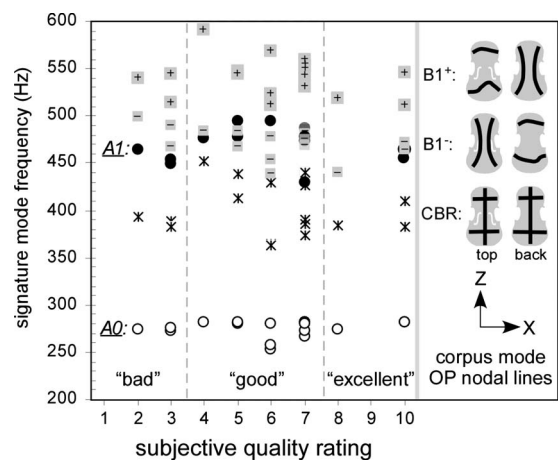

FIG. 3. Signature mode frequencies vs subjective quality rating for 17 violins: A0 (○), A1 (●); CBR (*), and B1$^-$ and B1$^+$ (shaded squares with − or +). Excellent violins all old Italian. Corpus mode OP nodal line patterns are on the right-hand side.

469 ± 19 Hz (430–494 Hz), CBR averaged 407 ± 31 Hz (363–452 Hz), B1$^-$ averaged 475 ± 16 Hz (439–500 Hz), and B1$^+$ averaged 541 ± 22 Hz (511–591 Hz).

The A1–A0 frequency ratio was 1.71 ± 0.05, in close agreement with values obtained for a rigid violin-shaped cavity.[15] An important coupling between A0 and A1 discovered in the rigid-cavity experiment reduces the expected Helmholtz-type A0 volume dependence significantly, providing the physical basis for the difficulty encountered by Hutchins and Schelleng in reliably scaling the violin octet "main air" resonance frequency to the various different pitch ranges by adjusting rib heights.[19]

Figure 3 shows no obvious quality-related trends in signature mode frequencies. The two bent wood violins (6,7 ratings) were unexceptional. Considering the remarkable range of frequencies for the 6- to 7-rated good violins, the only reasonable conclusion to be drawn from Fig. 3 is that signature mode frequencies are not robust quality indicators. Similar scrutiny of signature mode total damping, extracted by peak-fitting routines, also showed no robust quality indicators.

2. Damping trends

In an earlier report the frequency dependence of the total damping was investigated by isolating three-violin subsets of good and bad violin normal mode damping values from the mobility spectrum fits.[11] Power-law trend lines of the form $\zeta_{tot} = Cf^X$ were used to quantify damping falloff trends, with $x \approx -0.5$ seen for various structures.[20] Note that damping falloff for isolated top and back plates was consistent with $x \approx 0$, significantly slower than for the corpus.[9] Earlier analysis had shown a significant difference in x, with the good–bad exponent difference being 0.16 ± 0.07. Here the comparison, shown in Fig. 4, is between the *Plowden-Titian* and the bad violin data sets. The *Plowden–Titian* trend-line exponent, $x = -0.40$, was within error of the bad $x = -0.45 \pm 0.05$;[11] obviously total damping trends are *not* robust quality discriminators. Overall, total damping trends were similar for any violin quality class, with the earlier difference
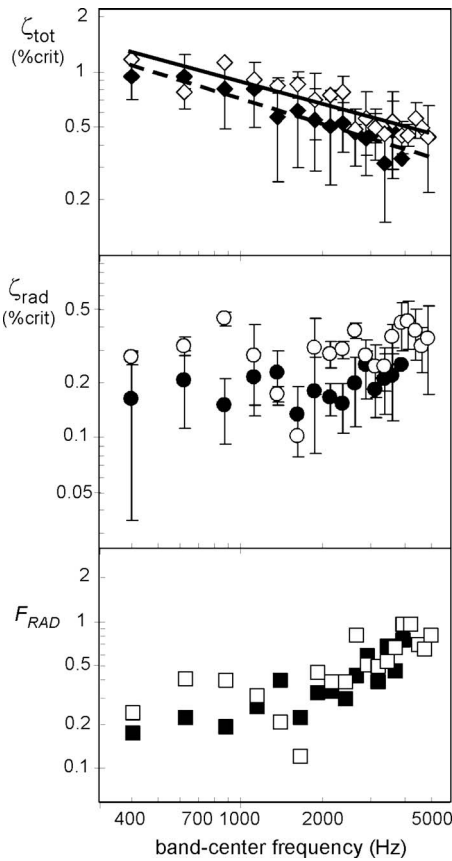
FIG. 4. Band-averaged (log) ζ_{tot} (top panel, with power law trend lines: Solid line "excellent," dashed line "bad"), (log) ζ_{rad} (middle panel), and (bottom panel) (log) F_{RAD} ($=\zeta_{rad}/\zeta_{tot}$) for excellent (open symbol) and bad (closed symbol) violin subsets vs (log) band-center frequency. *Intraband* s.d. error bars (top-middle); average F_{RAD} propagated errors (not shown) nominally $\pm 40\%$.

most likely due to the paucity of data. Note that even though the *Plowden-Titian* total damping values were within error of the bad violin values for any band below 4 kHz (with one exception), they were always slightly larger, primarily due to a radiation damping difference.

The radiation damping was computed from R_{eff} ($\zeta_{rad} \propto R_{eff}/fM$, where $M=$violin mass, $f=$mode or band-center frequency). R_{eff} plateaus above f_{crit}, creating a "knee" in the ζ_{rad} frequency dependence at f_{crit},[11] a maximum in the fraction-of-vibrational-energy-radiated $F_{RAD}=\zeta_{rad}/\zeta_{tot}$, and the most efficient region for vibration–sound conversion.

Since $\zeta_{tot}=\zeta_{rad}+\zeta_{int}+\zeta_{fix}\approx\zeta_{rad}+\zeta_{int}$ (*if* ζ_{fix} can be neglected), knowing ζ_{tot} and ζ_{rad} provides the only reliable path to computing ζ_{int} for internal (heat) losses in a structure. (The support fixture damping ζ_{fix} was $\leq 5\%$ of ζ_{tot} for our free–free suspension and therefore neglected.) However when the violinist holds the violin, ζ_{fix} *dominates* ζ_{tot}. Figure 4 shows excellent (*Plowden-Titian*) radiation damping higher than bad (although still with overlapping error bars) except for the 1375–1625 Hz bands. Lower ζ_{rad} values observed for bad violins are consistent with higher critical frequencies *and* higher violin mass. Bad violin masses were ~10% higher than excellent.

Higher excellent ζ_{rad} did lead to higher F_{RAD} values across the frequency span even though ζ_{tot} was also larger;

the difference was more apparent at the lower frequencies, essentially disappearing above 2 kHz, although propagated errors were so large ($\pm 40\%$) that little could be made of any difference. Interestingly, holding the violin makes support fixture damping (now the violinist!) dominate the total damping and leads to the violinist possibly perceiving a different situation when comparing excellent to bad violins; F_{RAD} decreases as expected (~50%), but the *relative difference* between violins increases.[9] Note that F_{RAD}—the "egress" filter for vibration–sound energy conversion—is completely independent of the "gatekeeper" filter, the violin bridge, which intermediates the initial vibrational string-corpus input energy transfer. It is an interesting "coincidence" that F_{RAD} peaks near those frequencies most strongly affected by bridge rocking mode frequency changes,[16] and where the ear is most sensitive.

The internal damping of the violin, $\zeta_{int}\approx\zeta_{tot}-\zeta_{rad}$, falls off with frequency somewhat faster than ζ_{tot} since ζ_{rad} increases slowly up to f_{crit}. Because internal damping is similar between these extreme violin quality classes—and propagated errors so large—no definite statement is possible. Practically speaking, at $f>3$ kHz, heat losses from air and surface absorption effects in a large auditorium—to say nothing of the expected violinist "support fixture" damping—are likely more important than internal damping.

3. R_{eff} and effective critical frequency

Due to its insensitivity to any shape-material properties of the vibrating object, R_{eff} becomes a very useful structural acoustics parameter to quantify vibration–radiation conversion. For a particular experimental setup, R_{eff} varies only with the ratio $\langle R^2\rangle/\langle Y^2\rangle$ for each mode, thus—guided by baffled piston radiation—implying an f^2 dependence and second-order polynomial trend line. Since violin shape and materials make accurate critical frequency estimates impossible, and the orthotropic nature of wood gives two values, *effective* critical frequencies f_{crit}, were estimated initially from experimental R_{eff} trend lines[11] solved for $R_{eff}=1$. Mode-to-mode R_{eff} varies widely, however, so that even in successive 250 Hz bands with two to four modes, substantial adjacent-band jumps were common, leading in turn to occasional unreliable second-order polynomial fits.

This difficulty was mostly circumvented by using band-averaged $\langle R\rangle/\langle Y\rangle$ plots to "linearize" the data; for the VIO-CADEAS setup f_{crit} was determined by solving the trend-line equation for $\langle R\rangle/\langle Y\rangle=35.2$ Pa s/m. Normally linear and second-order polynomial trend-line f_{crit} values were averaged. For f_{crit} values differing by more than 5%, an exponential trend-line value was added and the average recomputed.

The band-average $\langle R\rangle/\langle Y\rangle$ data for bad and excellent violins in Fig. 5 shows a distinct difference across the entire range, with the excellent linear trend line crossing the 35.2 Pa s/m line at ~3.5 kHz, while the bad trend line crosses near ~4.3 kHz, defining f_{crit} for each quality class. The overall average f_{crit} violin value, 3.9 kHz, was in good agreement with 4.5–4.9 kHz values computed by Cremer for

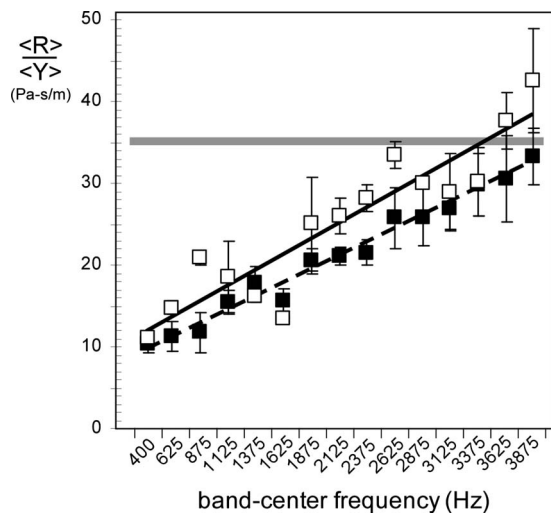George A. Bissinger: Structural acoustics good–bad violins

FIG. 5. Effective critical frequency estimates from 250 Hz band-averaged corpus $\langle R \rangle / \langle Y \rangle$ for two "excellent" (□) and three "bad" violins (■) vs band-center frequency, with linear trend lines (excellent, solid line, bad, dashed line). (s.d. error bars reflect *intraband* variations only). Lowest band center at 400 Hz. VIOCADEAS setup: f_{crit} ($R_{eff}=1$) at $\langle R \rangle / \langle Y \rangle$ = 35.2 Pa s/m (broad gray line).

violin-size flat rectangular spruce and maple wood plates (cross-grain), with along-grain f_{crit} values two octaves higher.[21]

A dip near 1625 Hz, a universal aspect of violin R_{eff} curves, is suggestive of a link to the ring frequency for cylinders,[20] for violins nominally 1 kHz.[13] Relative prominence for this band is associated with "nasality" in the overall tone. Higher excellent violin ζ_{rad} in Fig. 4 follows directly from increased $\langle R \rangle / \langle Y \rangle$ and the resultant lower f_{crit}, in combination with lower mass.

A plot of f_{crit} versus quality rating for 14 violins is presented in Fig. 6. Looking only at bad versus excellent violins, a case might be made that there is a significant difference between these classes, but the best of the good violins show a range encompassing these quality extremes, again undermining any robust quality-related trend. Note also that machine-figured plates in factory violins typically run significantly thicker than these tested bad violins, implying a lowered critical frequency.

4. Directivity

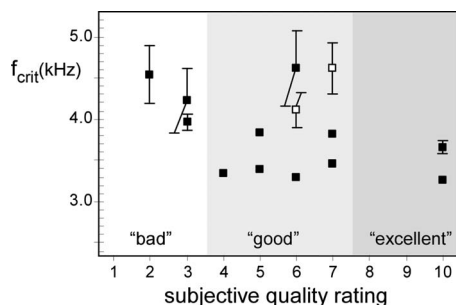Although Fig. 2 showed little difference in averaged-over-sphere radiativity between bad and excellent violins, the

FIG. 6. f_{crit} vs subjective quality rating for 14 violins (□—bent wood violins, all others carved plates). (s.d. errors reflect variation between various trend-line estimates only; point size hides smallest errors.)
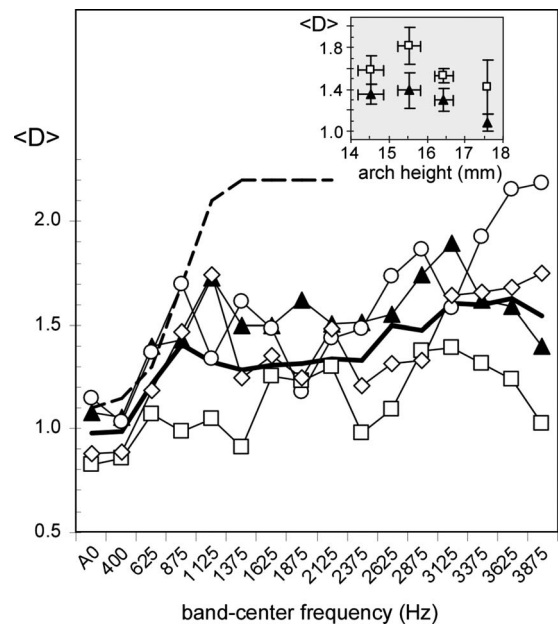
FIG. 7. Directivity for "bad" (▲), *Titian* (○), *Plowden* (◇), *Willemotte* (□), and 17-violin average (thick line) vs frequency. Directivity of *f*-hole radiation only (Ref. 10) shown as dashed line. *Titian* had highest $\langle D \rangle$, *Willemotte* had the lowest. Nominal intraband variations 15%. [Inset: Average $\langle D \rangle$ for 625–875 Hz (▲) and 3125–3875 Hz (□) regions vs arch height for 17 violins; s. d. error bars.]

way the violin is always held by a soloist implies that violin sound directionality must be an important facet of being heard over the orchestra. The violinist would be expected to hold the violin in the way that most effectively gets the sound to the audience, implying the top radiates more effectively than the back. The sound from the back also effectively has two extra (floor–back wall) bounces before heading into the hall, further diminishing its importance. The directivity $\langle D \rangle = \langle R_{top} \rangle / \langle R_{back} \rangle$ summarized for all 17 violins in Fig. 7 is a simple measure of sound directionality. Bad violin $\langle D \rangle$ generally was above the 17-violin average; the *Titian* had the highest $\langle D \rangle$ overall of any violin tested to date (with one bad violin quite close) and the *Willemotte* the lowest, while the *Plowden* was very close to average. Obviously directivity varies widely, even among the violins of one maker, with no link to perceived quality.

Figure 7 highlights an unexpected behavior, viz., the surprisingly fast rise of $\langle D \rangle$ at 625–875 Hz (followed by a plateau from 1 to 2.5 kHz, then a slow rise above 2.7 kHz). In the 625–875 Hz region where $\lambda \geq$ violin size, $\langle D \rangle \approx 1$ (isotropic) radiation would be expected. A reasonable interpretation of this rapid rise, based on recent "patch" NAH results for just *f*-hole radiation[10] compared to the anechoic chamber measurements of corpus+*f*-hole radiation, is based on the fact that *f*-hole-only radiation contributed ∼50% to the overall violin radiation at $f < 1$ kHz (falling off with increasing frequency) *and* was significantly more directional at lower frequencies (dashed line, Fig. 7) than expected, e.g., if the 625 or 875 Hz bands had a 50–50 *f*-hole-corpus radiation balance, then the amalgamated $\langle D \rangle$ would be $(1.3+1)/2 \approx 1.2$, or $(1.8+1)/2 \approx 1.4$, respectively, close to 17-violin values.

Does arching affect directivity? The *Willemotte* top plate arching of 17.6 mm was highest of all violins tested (along with the Curtin violin), while the *Plowden* was the next-to-lowest at 14.1 mm. CT scan bridge slices were used to estimate arch heights ±0.3 mm; Curtin and Zygmuntowicz violins had directly measured values. Arching groups of 14 to 15 mm (seven violins), 15 to 16 mm (three violins), 16 to 17 mm (five violins), and 17 to 18 mm (two violins) were plotted versus average $\langle D \rangle$ in the 625–875 and 3125–3875 Hz bands to create the inset in Fig. 7. Overall, the highest arch violins appear to have lower overall directivity, with the suggestion of a maximum in the 15 to 16 mm range. However, real arching effects might be entangled with OP–IP differences that also imply a directivity link.

C. Three-dimensional modal analyses

The 3D modal analyses examined a difficult and hence neglected area of violin vibratory behavior, viz. out-of-plane flexural versus in-plane extensional motion. The fundamental coupling between flexural and extensional motion, combined with possible transformations of extensional into flexural motion—and vice versa—at edges (e.g., rib joints) and discontinuities (e.g., bass bar, *f* holes, soundpost), make this an extraordinarily difficult analytic problem for complicated structures. However, experimentally determining the relative importance of flexural versus extensional motion is a promising avenue for understanding violin radiative properties at a fundamental level. These measurements investigated two important aspects of violin sound: (1) how OP–IP vibrational energy partitioning might affect violin radiation, and (2) how violin corpus motion immediately in the vicinity of the bridge feet might relate to string energy transfer through the bridge feet to the corpus.

1. OP–IP vibrations and directivity

OP mobility extracted from 3D scans was shown in Fig. 1 for the *Titian* and *Plowden*. The magnitudes were similar to those of other violins. Of more interest here is the strength of OP relative to IP motions. Since only the OP component is responsible for radiation, the reasoning here—assuming the same averaged overall magnitude—is that larger OP/IP ratios should correlate with more sound production. Figure 8 presents OP/IP ratios for the top plate and back plates of all violins with 3D scans, even partial ones. Three maple backs all had similar OP/IP ratios, implying a constant radiative contribution, while the top plate OP/IP—with varied-geometry bass bars and *f* holes—differed significantly. (Violin-making lore has long stressed the relative importance of the top versus back to violin sound.)

Maple backs had much higher OP/IP ratios than spruce tops, and the *Titian* top plate had a much higher ratio than either the *Plowden* or Curtin violins. Also included in Fig. 8 was the measured directivity for the *Titian* and *Plowden*. The higher OP/IP ratio for the *Titian* was accompanied by higher directivity compared to the *Plowden*; the Curtin violin directivity was similar to the *Plowden* (both near average) and consistent with its top OP/IP ratio, and the assumption of a relatively constant ratio for the back. Moreover, an arching-
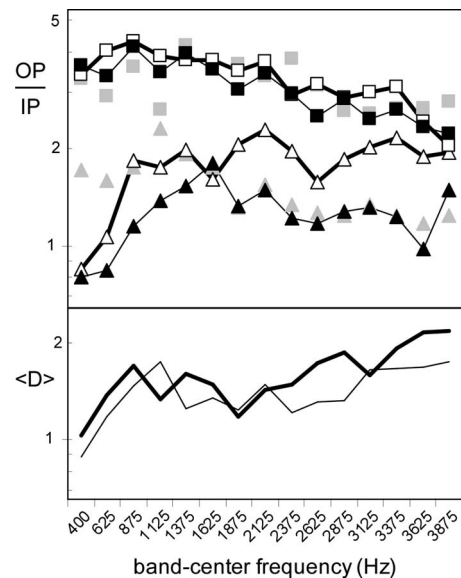

FIG. 8. Top panel: OP/IP (log) mobility ratio vs band-center frequency. Top plate—△ (*Titian*, open, thick line; *Plowden*, filled, thin line; Curtin, gray); back plate—□ (*Titian*, open, thick line); *Plowden*, filled, thin line; *Willemotte*, gray). Bottom panel: (log) directivity: *Titian* (thick line), *Plowden* (thin line).

directivity correlation, if real, offers a possible link to the OP/IP ratio depending on arching also. Of course, the flat plate (arch=zero) has only OP motion to first order, and thus a very high OP/IP ratio.

2. OP–IP, BH, and the bridge island

One poorly understood aspect of violin vibrations is the origin of the BH peak near 2.4 kHz in the OP mobility *and* accompanying radiativity spectra (Fig. 2). This structure seems unusual only because of its magnitude, with typical R_{eff} and ζ_{tot} values for its frequency region. Bridge rocking about the waist leading to up–down antiphase bridge feet motions that excite corpus OP motion have been proposed as a physical mechanism for this peak.[22,23] Examination of OP motion near 2.4 kHz, however, indicated little such antiphase motion at the bridge feet, although as noted a significant peak in OP motion was observed in $\langle Y_{\text{corpus}} \rangle$.

The BH peak has shown some sensitivity to changes in the bridge rocking mode frequency f_{rock}, especially at f_{rock} values closest to 2.4 kHz, where its amplitude and centroid frequency slumped noticeably (cf. Fig. 10, Ref. 16). This experimental observation links the BH peak with the bridge, but does not lead to an obvious explanation of the underlying mechanism. Understanding this region is crucial because string energy enters the corpus here through a tuned sub-structure whose optimized coupling to the corpus is essential to good violin sound[16] *and* because abundant nearby boundaries–discontinuities—especially so in the *X* direction—create a favorable environment for extensional →flexural transformations that can lead to acoustic radiation.

If bridge rocking motions do not produce the BH peak what does? Durup and Jansson, in a systematic "violin" experiment using a simplified geometry violin (flat rectangular plates), observed a BH peak only *after* cutting simplified *f*
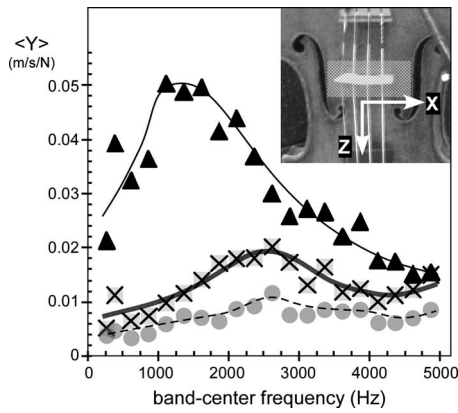
FIG. 9. Three-violin-average three-dimensional bridge-island rms mobilities vs band-center frequency (lines drawn to guide eye only): $\langle Y_Y \rangle$—▲ (thin solid line), $\langle Y_X \rangle$—⊠ (thick solid line), $\langle Y_Z \rangle$—● (without Curtin violin- see the text; thin dashed line). Nominal intra-band s.d. $\approx \pm 0.007$ for $\langle Y_Y \rangle$ and $\langle Y_X \rangle$. (Inset: Hatched bridge-island region superimposed on violin photo with X–Z axes notated.)

FIG. 10. Impedance ratio of bridge (1D) to bridge island (3D) vs band-center frequency for Y(■) and X(⊠) directions. (Inset: Bridge point measurement location–direction).

holes (three-segment, squared-off, elongated "S" shapes) into the top plate. Crucially, only the long straight section led to the BH peak *and* no BH peak appeared when this section was above the bridge.[17] If cutting f holes is essential to creating both a bridge island and the BH peak, perhaps the simultaneous reduction in X direction stiffness around the bridge feet *and* creation of close-by boundaries–discontinuities offers a plausible augmenting mechanism for OP motion, viz. an alternative IP bridge→corpus →radiation path via extensional→flexural transformation with substantial subsequent radiation.

The 3D measurements also allowed us to investigate IP motions along X and Z directions directly. Mobilities were rms averaged over 19 points in a small region of the top plate near the bridge feet—a bridge island, here shown as an inset in Fig. 9 with X and Z axes noted. The island X-Y-Z mobility components (notated as $\langle Y_X \rangle$, $\langle Y_Y \rangle$, $\langle Y_Z \rangle$) for the *Plowden, Titian*, and Curtin violins were band-averaged separately, rather than having the X and Z components conglomerated into an overall IP motion as before.

The *Titian–Plowden*–Curtin three-violin-average bridge-island 3D mobility behaviors shown in Fig. 9 present some interesting differences from the corpus mobility (OP) results in Fig. 2:

(1) The $\langle Y_Y \rangle$ peak is now near 1.4 kHz, not 2.5 kHz as seen in Fig. 2, with a relatively smooth falloff above this.
(2) $\langle Y_Z \rangle$ is overall the lowest across the range, while $\langle Y_Y \rangle$ is the highest, likely reflecting relative stiffnesses along each direction, and possibly even the X-direction excitation at the bridge corner.
(3) $\langle Y_X \rangle$ has a definite, broad peak near 2.5 kHz, and was the only mobility component to show a definite peak in the BH region.
(4) $\langle Y_X \rangle$ for the *Plowden* was close in magnitude ($\sim 70\%$) to $\langle Y_Y \rangle$ near 2.4 kHz, with the *Titian* being much lower ($\sim 30\%$).
(5) From 625 to 4875 Hz the *Titian* $\langle Y_Y \rangle / \langle Y_X \rangle$ ratio is about twice the *Plowden* and Curtin values. It is quite possible
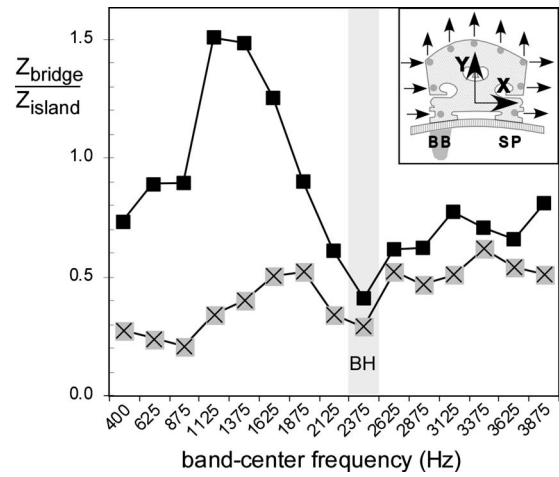
this difference reflects the OP/IP corpus ratio and directivity results presented in Fig. 8.
(6) The Curtin violin results were quite similar to those of the *Plowden*, with comparable $\langle Y_Y \rangle$ (and $\langle Y_X \rangle$) magnitudes and trends. The $\langle Y_X \rangle$ peak was broader than for either old Italian; $\langle Y_Z \rangle$ was too weak-noisy for reliable analysis and was not included in Fig. 9.

The presence of the bridge-island $\langle Y_X \rangle$ peak near 2.5 kHz for the three-violin average suggests significant X-plane motion accompanying bridge rocking motion in string-corpus energy transfer. Unfortunately, there were no bridge 3D measurements. Accordingly the 12-violin 1D bridge measurements were reanalyzed to look at X and Y bridge motions separately, and then used in conjunction with 3D bridge-island results to compute a bridge/bridge-island impedance ratio.

The bridge 1D rms mobility results had previously shown a prominent BH peak when averaged over X and Y mobilities;[16] reanalysis of X (side-only) and Y (top-only) measurements (see Fig. 10 inset for point locations–directions) showed ~ 2.4 kHz peaks in rms mobility for both directions separately. Since string→bridge→bridge-island energy transfer is so important, a rough measure of direction-specific impedance relationships based on mobility average inverses was used to compute the X and Y impedance ratios, Z_{bridge}/Z_{island}, separately. These ratios, presented in Fig. 10, show a distinct local minimum in the BH region for X and Y directions, as well as a prominent maximum near 1.3 kHz for the Y direction. The trends seen in Figs. 9 and 10 are certainly suggestive of some bridge to bridge-island excitation mechanism based on X motion.

One additional, possibly pertinent note related to the old Italian CT scans was that all these violins showed some significant internal repair work around the bridge region where the soundpost and bridge feet (and bass bar replacement) tend over time to disrupt the structural integrity of the soft spruce top plate (Fig. 11). Localized repairs in this critical
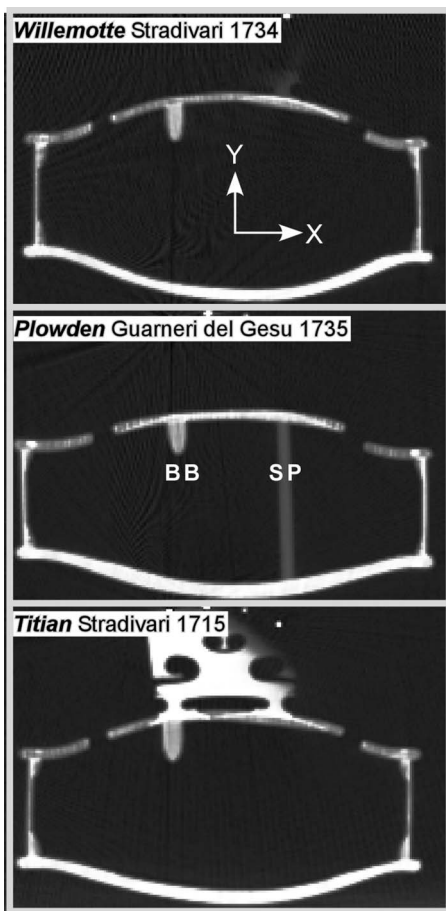
J. Acoust. Soc. Am., Vol. 124, No. 3, September 2008

George A. Bissinger: Structural acoustics good–bad violins   1771

FIG. 11. CT scan slice in the bridge-soundpost region of three old Italian violins. Repairs under bridge feet in spruce top ($\rho \approx 0.4$ g/cm^3) over bass bar and soundpost are readily seen as higher-density (brighter) regions. (Maple back and bridge have $\rho \approx 0.6$ g/cm^3.)

energy transfer region are a natural companion to age and playing, and are universal to instruments of the classical period.

These repairs commonly require gluing in wood patches. If the patch density matched the original, and the fit were flawless only the (brighter) higher density glue-line arc would stand out in a CT scan. Standing out among these violins, the *Titian* also showed an additional, small high density patch underneath the bass bar-side bridge foot, as well as a prominent patch glue line under the soundpost-side bridge foot. Whatever the cause of the *Titian*'s high OP–IP ratio, these repairs are mentioned because of extensional →flexural transformations possible at discontinuities. Perhaps density discontinuities at a patch glue line could be one such cause?

IV. CONCLUSIONS

Examining the totality of our experimental results for violins of widely varying quality it was impossible to reach a conclusion different than that of previous researchers, viz. that the very best violins *measure* little different from the worst (assuming all had been properly setup, of course). All had similar underlying structural acoustic behaviors: signature modes with unexceptional frequencies and total damping, total damping trends, radiation efficiency trends, fraction

of vibrational energy turned into sound, etc., etc. What was observed were different spectral balances as the relative magnitudes of various psychoacoustically important regions changed over the profiles, perhaps tilting toward the low or high ends of the profile, or emphasizing a specific region. (Schleske has commented extensively on the effects of such shifts/emphases in spectral balance on perceived sound quality.[24])

The excellent violin radiativity profiles do reflect common remarks about the best violins—they are more "even" across the measured range, and strong in the lowest range. As to being loud? In a large auditorium where typical reverberation provides a low frequency boost and a high frequency rolloff above 5 kHz, the BH+bridge+F_{RAD} concentration of sound near 2–4 kHz (where the ear is most sensitive) combined with the higher frequency directivity "boost" seen for the *Titian* (but not the *Plowden* or *Willemotte*) could certainly help a solo violin being heard over the orchestra.

Can our experimental modal–acoustic results address such matters as pretreating wood with various chemicals, or deal with the varnish per se? Succinctly, no. Assuming constant shape, violin response to some driving force is determined by the overall stiffness-density properties of its various materials, irrespective of how these were arrived at. At this time the most productive area scientifically appears to be the radiativity profile, the "measureable" at the end of the energy trail that seems most immediate to a violinist in the overall judgment of violin sound quality. Structural acoustics modeling of the entire profile offers significant additional insight into quality-related differences.

Perhaps a contrarian viewpoint about quality might be useful here? What truly defines violin excellence? If the answer is truly excellent violinists, then the reliability-reproducibility of their psychoacoustic judgments must draw more attention. It would seem illogical to expect violinists who pride themselves on their personal sound not to prefer certain violins over others because they are better at creating that sound. If excellent violinists cannot agree on a quality rating because of sound preferences—or worse, rate two quite different sounding violins as good—shouldn't it follow that scientific measurements could do no better?

[1]K. D. Marshall, "Modal analysis of a violin," J. Acoust. Soc. Am. **77**, 695–709 (1985).
[2]G. Bissinger, "Some mechanical and acoustical consequences of the violin soundpost," J. Acoust. Soc. Am. **97**, 3154–3164 (1995).
[3]M. Schleske, "Eigenmodes of vibration in the working process of a violin," Catgut Acoust. Soc. J. **3**, 2–8 (1996).
[4]M. Schleske, "On making 'tonal copies' of a violin," Catgut Acoust. Soc. J. **3**, 18–28 (1996).
[5]M. Schleske, "Empirical tools in contemporary violin making. 1. Analysis of design, materials, varnish and normal modes," Catgut Acoust. Soc. J. **4**, 50–65 (2002).
[6]G. Bissinger and A. Gregorian, "Relating normal mode properties of violins to overall quality: Signature modes," Catgut Acoust. Soc. J. **4**, 37–45 (2003).
[7]G. Bissinger, "Modal analysis of a violin octet," J. Acoust. Soc. Am. **113**, 2105–2113 (2003).
[8]G. Bissinger and J. C. Keiffer, "Radiation damping, efficiency, and directivity for violin normal modes below 4 kHz," Acoust. Res. Lett. Online **4**, 7–12 (2003).
[9]G. Bissinger, "Contemporary generalized normal mode violin acoustics," Acust. Acta Acust. **90**, 590–599 (2004).
[10]G. Bissinger, E. G. Williams, and N. Valdivia, "Violin *f*-hole contribution to far-field radiation via patch near-field acoustical holography," J. Acoust. Soc. Am. **121**, 3899–3906 (2007).
[11]G. Bissinger, "The role of radiation damping in violin sound," ARLO **5**, 82–87 (2004).
[12]A. Runnemalm, N. E. Molin, and E. Jansson, "On operating deflection shapes of the violin body including in-plane motions," J. Acoust. Soc. Am. **107**, 3452–3459 (2000).
[13]G. Bissinger, "A unified materials-normal mode approach to violin acoustics," Acust. Acta Acust. **91**, 214–228 (2005).
[14]D. E. Oliver, V. Palan, G. Bissinger, and D. Rowe, "3-dimensional laser doppler vibration analysis of a stradivarius violin," *Proceedings of the 25th International Modal Analysis Conference, Society for Experimental Mechanics*, Bethel, CT, 2007, paper 372 (CD proceedings only).
[15]G. Bissinger, "A0 and A1 coupling, arching, rib height, and *f*-hole geometry dependence in the 2-degree-of-freedom network model of violin cavity modes," J. Acoust. Soc. Am. **104**, 3608–3615 (1998).
[16]G. Bissinger, "The violin bridge as filter," J. Acoust. Soc. Am. **120**, 482–491 (2006).
[17]F. Durup and E. Jansson, "The quest of the violin bridge-hill," Acust. Acta Acust. **91**, 206–213 (2005).
[18]E. Rohloff, "Ansprache der Geigenklänge (The speaking of violin sounds)," Z. Angew. Phy. **17**, 62–63 (1964). English abstract published in *Musical Acoustics, Part II, Violin Family Functions*, Benchmark Papers in Acoustics, Vol. **6**, edited by C. M. Hutchins (Dowden, Hutchinson & Ross, Stroudsburg, PA, 1976).
[19]C. M. Hutchins, "A 30-year experiment in the acoustical and musical development of violin-family instruments," J. Acoust. Soc. Am. **92**, 639–650 (1992).
[20]F. Fahy and P. Gardonio, *Sound and Structural Vibration: Radiation, Transmission and Response*, 2nd ed. (Academic, New York, 2007).
[21]L. Cremer, *The Physics of the Violin* (MIT, Cambridge, 1984).
[22]I. P. Beldie, "About the bridge hill mystery," Catgut Acoust. Soc. J. **4**, 9–13 (2003).
[23]J. Woodhouse, "On the bridge-hill of the violin," Acust. Acta Acust. **91**, 155–165 (2005).
[24]M. Schleske website, http://www.geigenforschung.de/11handbuch/en_extras3handbuch04klangfarbe.pdf. (last viewed 15 May, 2008).